Interferometric and localized surface plasmon based fiber optic sensor

Interferometric and localized surface plasmon based fiber optic sensor

Harald Ian D. I. Muri, Andon Bano, Dag Roar Hjelme

Harald Ian D. I. Muri, Andon Bano, Dag Roar Hjelme, "Interferometric and localized surface plasmon based fiber optic sensor," Proc. SPIE 10058, Optical Fibers and Sensors for Medical Diagnostics and Treatment Applications XVII, 100580F (28 February 2017); doi: 10.1117/12.2250743

SPIE.

Event: SPIE BiOS, 2017, San Francisco, California, United States

Interferometric and localized surface plasmon based fiber optic sensor

Harald Ian D.I. Muri[a], Andon Bano[a], and Dag Roar Hjelme[a]

[a]Norwegian University of Science and Technology, Gunnerus gate 1, Trondheim, Norway

ABSTRACT

We demonstrate a novel single point, multi-parameter, fiber optic sensor concept based on a combination of interferometric and plasmonic sensor modalities on an optical fiber end face. The sensor consists of a micro-Fabry-Perot interferometer in the form of a hemispherical stimuli-responsive hydrogel with immobilized gold nanoparticles. We present results of proof-of-concept experiments demonstrating local surface plasmon resonance (LSPR) sensing of refractive index (RI) in the visible range and interferometric measurements of volumetric changes of the pH stimuli-responsive hydrogel in near infrared range. The response of LSPR to RI ($\frac{\Delta\lambda_r}{\Delta \mathrm{RI}} \sim$ 877nm/RI) and the free spectral range (FSR) to pH ($\frac{\Delta \mathrm{pH}}{\Delta \mathrm{FSR}} = 0.09624/\mathrm{nm}$) were measured with LSPR relatively constant for hydrogel swelling degree and FSR relatively constant for RI. We expect this novel sensor concept to be of great value for biosensors for medical applications.

Keywords: Fiber optic sensors, smart hydrogel, hydrogel, LSPR, nanoplasmonics, multiparametric sensor

1. INTRODUCTION

Multiplexed fiber optic sensors often utilize one single point for one sensing parameter and another single point for another sensing parameters. The sensing parameter is often based on optical or photonic features like attenuation of light, Fiber Bragg Gratings (FBG), or interferometric cavities. However, in some applications as in the medical field, there is a great need for many sensing parameters in one single point. Attractive attributes among medical sensors are label-free sensing, small dimensions, real-time monitoring and high sensitivity. Fiber optic sensors can fulfill many of these requirements by exploiting intrinsic or extrinsic light-matter interactions at the side-face or end-face of an optical fiber (OF). Localized surface plasmon resonance (LSPR) that noble metal nanoparticles (NMNO) exhibit have shown to have promising optical properties for label-free sensing. The label free sensing can also be multiparametric by spectrally resolving different LSPR that is observed for different NMNP of size and shape.[1] Single point fiber optic (FO) LSPR based sensors proposed over the last decade have LSPR interacting with evanescent field around the fiber core or with the light at the fiber end-face.[2,3] The use of fiber end-face as a sensor design offers simpler manufacture methods as compared to utilizing the side face since the sensor design is less dependent on the removal of cladding and the steps involved in the surface preparations. Previous work from our group demonstrated a proof-of-concept fiber optic pH sensor based on the reflection of spherical gold nanoparticles (GNP) embedded in acrylamide hydrogel at the fiber end-face.[4] In this paper, we are combining the LSPR of gold nanorods (GNR) in visible (VIS) range with the interferometric measurements of pH stimuli responsive hydrogel volume in infrared range (IR) in an effort to utilize two label free sensing parameters in one single point. The use of GNR have several advantages over spherical GNP such as increased stability, high response to refractive index and two LSPR peaks that can be used for sensing. The crosstalk is expected to be small between the LSPR signal and interferometric signal since they are recorded at different spectral bands and since light-matter interactions are localized at the order of nanometer for LSPR and at the order of micrometer for the Fabry-Perot (FP) interferometer. A double cladded optical fiber (DCOF) propagate the reflection of the VIS LSPR and the IR interferometric signal. The large core of the DCOF propagate the reflected LSPR signal in multimode (MM) while the small core propagate the reflected interferometric signal in

Further author information: (Send correspondence to Harald Ian Muri)
Harald Ian Muri: E-mail: harald.muri@ntnu.no, Telephone: +4773412688
Dag Roar Hjelme: E-mail: dag.hjelme@iet.ntnu.no, Telephone: +4773559604
Andon Bano: E-mail: andonb@stud.ntnu.no, Telephone: +393209450050

Optical Fibers and Sensors for Medical Diagnostics and Treatment Applications XVII, edited by Israel Gannot,
Proc. of SPIE Vol. 10058, 100580F · © 2017 SPIE · CCC code: 1605-7422/17/$18 · doi: 10.1117/12.2250743

single mode (SM). The LSPR peak position is in this paper measured as a function of bulk RI controlled with glycerol or sucrose while FSR is measured as a function of the poly(acrylamide-co-acrylic acid)(pAAMAAC) hydrogel swelling degree stimulated by pH solutions. Acrylic acid is a co-monomer in the polymer network and is deprotonated or protonated with certain pH resulting in influx or outflux of water in the hydrogel, respectively. The FO sensor is then also demonstrated as a pH and RI sensor. The fiber optic setup made in this paper can also be used in applications such as real-time monitoring of specific markers for critical ill patients under or after surgery.[5,6] Results from the proof-of-concept experiments presents LSPR sensing of refractive index (RI) in the visible (VIS) and interferometric measurements of volumetric changes of the stimuli-responsive hydrogel in the infrared (IR) range. The hemispherical hydrogel at the fiber end face represents a low-finesse FP etalon where the optical length is read out as a measure of the stimuli responsive hydrogel volume. The GNR immobilized in the hydrogel have a LSPR peak with properties similar to a damped lorentzian and the peak position is dependent on the local RI surrounding the GNR. The spectral response of the FP etalon and LSPR as a function of hydrogel volume and RI, respectively, are illustrated in figure 1.

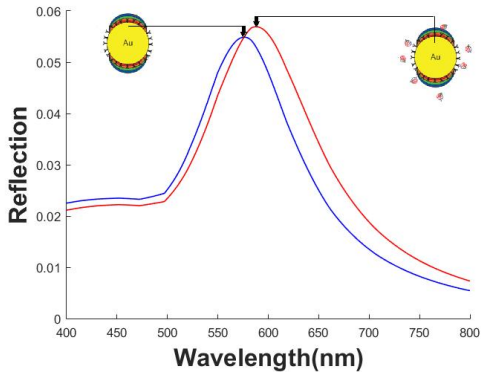

(a) Illustration of the spectral response of the LSPR sensing. Simulation from Mie solutions in Matlab

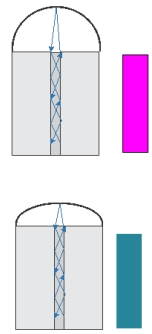

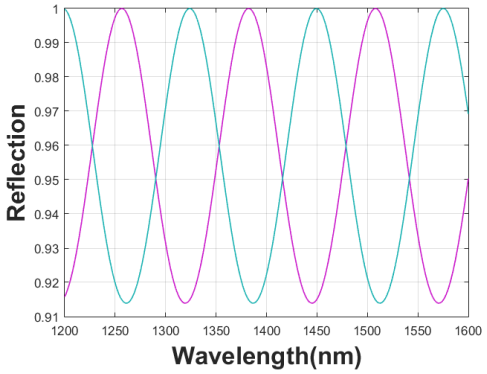

(b) Illustration of the spectral response of the sensing with hydrogel as FP etalon. Simulation from FP-etalon equations in matlab.

Figure 1: Illustration of the spectral response of the LSPR and FP etalon of GNR immobilized in hydrogel

The hydrogel at the fiber end-face reflects light at the gel-solution r_2 and the fiber-gel r_1 interfaces. Multiple reflections of IR light is neglected because of low reflectivity at the gel-solution interface. The total IR reflection of the hydrogel at OF can therefore be described as the sum of two monochromatic waves of the same wavelength λ and complex amplitudes but with different phase. The two waves can be expressed as, $\mathrm{U}_1 = \sqrt{\mathrm{I}_0 r_1}\exp(-ikz)$ and $\mathrm{U}_2 = \sqrt{\mathrm{I}_0 r_2 \gamma}\exp(-i(k(z-2l_0)-\varphi_0))$, where $k = \frac{2\pi}{\lambda}$, l_0 is the optical length of the gel cavity, γ is loss factor (absorption, scattering, mode mismatch), z is the propagating direction of the wave and φ_0 is the initial arbitrary phase. Explicitly, the sum of U_1 and U_2 results in the intensity,

$$\mathrm{I}_3 = \mathrm{I}_0\left[\mathrm{r}_1{}^2 + (\gamma \mathrm{r}_2)^2 + 2\gamma \mathrm{r}_1 \mathrm{r}_2 \cos(\frac{4\pi l_0}{\lambda} + \varphi_0)\right] \tag{1}$$

A change in $l_0 = l n_{\mathrm{gel}}$ may originate from the RI in the gel or simultaneously, from a change in the physical length l of hydrogel cavity,

$$\Delta l_0 = \Delta l n_{\mathrm{gel}} + l\Delta n_{\mathrm{gel}} \tag{2}$$

where n_{gel} is the RI of the gel originating from the solution or the polymer concentration (swelling degree of hydrogel). The interferometric measurements were carried out by recording the free spectral range (FSR) of the reflected IR spectrum. FSR for wavelength is found when I_3 is at maximum $\rightarrow \frac{4\pi l_0}{\lambda_0} + \varphi_0 = q2\pi$, for positive integers of q=0, 1, 2, ..., leading to,

$$\Delta\lambda = \frac{\lambda_0{}^2}{2l_0} \tag{3}$$

where λ_0 is the center wavelength of the light source. Similar to previous work, change of FSR or phase of the interferometric spectrum can be read out and subsequently the change of the optical length computed.[5]

The absorption and scattering of incident light on metallic nanostructures depends on the light frequency, size, shape, the dielectric environment, and the material composition. The optical properties of noble metal nanorods can be described by Gans theory that is a generalization of Mie theory for spheroidal particles where their extinction spectrum exhibit two peaks, one corresponding to the transverse plasmon mode and one corresponding to the longitudinal plasmon mode.[1] The reflection from GNR in acrylamide hydrogel at the OF end-face have an extinction cross section coefficient that is the sum of the scattering and the absorption cross section coefficient. For a dipole this extinction cross coefficient is maximized when the real dielectric function of gold nanoparticle $\varepsilon_1(\lambda)$ and dielectric constant of medium ε_m have the relation

$$\varepsilon_1(\lambda) = -2\varepsilon_m \tag{4}$$

that shows LSPR to be dependent on the dielectric constant of the medium. For small range of refractive index n_m Drude model also express the LSPR peak position with corresponding wavelength as

$$\lambda_{\max} = \lambda_p \sqrt{2{n_m}^2 + 1} \tag{5}$$

where λ_p is the plasma oscillation frequency of the bulk metal.[7] As LSPR depends on the dielectric constant of the medium, label free sensing is possible by surface functionalizing the GNR with receptors that can selectively bind to specific biomolecules where a recombination of receptor-biomolecule is red shifting the LSPR peak position.

2. MATERIALS AND METHODS

The fiber optic sensor have been fabricated as described from previous work.[4] In this paper citrate stabilized 670nm resonant GNR (50OD, $1.14 \cdot 10^{13}$ particles/mL, nanoCompix) were used to make pregel solutions of 10wt% Acrylamide (AAM)-Acrylic acid (AAC) (molar ratio 1/2 AAM/AAC) and 2 mol% N,N-methylenebisacrylamide (BIS). Hydrochloric acid (HCL) (1.0M, Sigma Aldrich) and sodium hydroxide (NaOH) (1.0M, Sigma Aldrich) were added to mq water to prepare pH solutions to stimulate a change in volume of the hydrogel. Glycerol (>99%, VWR) or Sucrose (>99.5%, VWR) were added to mq water to prepare RI solutions to shift the LSPR peak position. The fiber optic (FO) instrument illustrated in figure 2 consist of following components; light source 1 (MBB1F1, 470-850nm, Thorlabs), light source 2 (S5FC1005S, 1550nm, 50nm bandwidth, Thorlabs), 2x2 coupler multimode (MM) (50/50, FCMH2-FC, 400-1600nm, Thorlabs), 2x2 coupler single mode (SM) (50/50, 84075633, 1550nm, Bredengen), doubled cladded optical fiber (DCOF) 2x2 coupler (DC1300LEB, MM 400 - 1600 nm, SM 1250 - 1550 nm, Thorlabs), spectrometer 1 (QE65Pro, Ocean Optics), spectrometer 2 (NIRQuest-512-1.7, Ocean Optics), loose fiber-end terminated with index matching gel (G608N3, Thorlabs), sensor segment of Ø125 μm DCOF (DCF13, Thorlabs), program Spectrasuite (Ocean Optics). Optical fibers (OF) were connected using a Fitel Fusion Splicer (Furukawa Electric).

2.1 Reflection measurements of GNR embedded in hydrogel in VIS and IR

Due to the perturbations in the pAAMAAC hydrogel that creates artifacts in the reflected LSPR signal the VIS spectrum of the hydrogel without the GNR were recorded and used as reference for each of the solutions containing certain pH and glycerol or sucrose concentration. Reference spectra for the IR was recorded from the reflections of the bare DCOF in mq water solution. The dark spectrum was recorded with minimal light from surroundings and with the light source turned off. The following relation of the reflection was used to obtain the spectrum,

$$I_{\mathrm{R}} = \left(\frac{S_\lambda - D\lambda}{R_\lambda - D_\lambda}\right) \cdot 100\% \tag{6}$$

where I_{R} is reflection spectra, S_λ sample spectra, R_λ is reference spectra, and D_λ is the dark spectra. The hydrogel swelling/deswelling with and without GNR was induced by dipping the gel-fiber into pH solutions at

4.5, 4.25, 4.0, 3.75 and 3.5. The RI solutions consist of glycerol and sucrose with bulk RI between 1.3301 and 1.3848. The reference and sample spectra were recorded after the hydrogel swelling/deswelling had reached equilibrium. pH was controlled with pH meter (inoLab pH/ION 7320, WTW), pH electrode (pHenomenal MIC 220, VWR Collection), and temperature sensor (pHenomenal TEMP21, VWR Collection). All experiments were carried out at room temperature. HCl or NaOH were added to mq water to prepare pH solutions while glycerol or sucrose was added to mq water to prepare RI solutions. The bulk RI values from different wt% of glycerol and sucrose in mq water were obtained from Handbook of Chemistry and Physics at λ=589nm.[8]

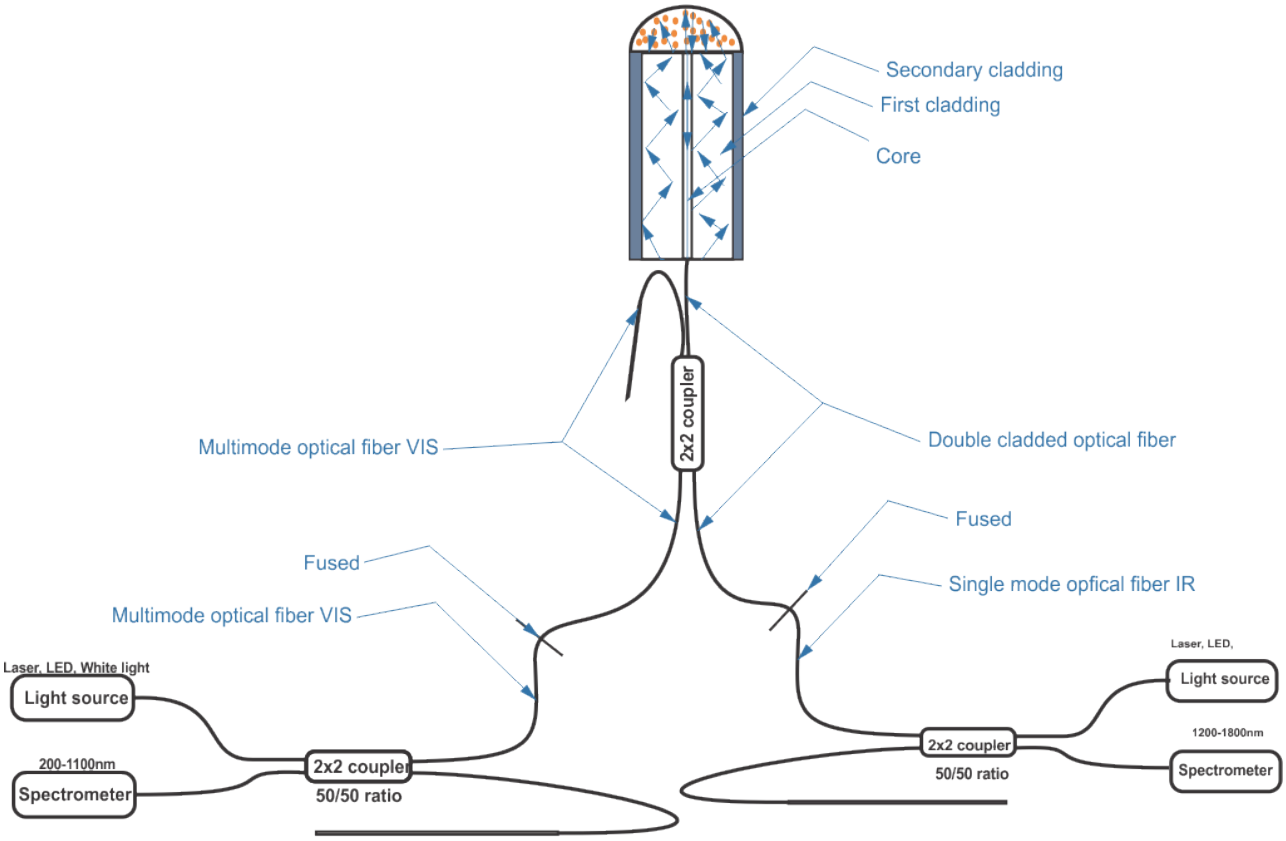

Figure 2: Set up of the fiber optic instrument based on reflection measurements

3. RESULTS AND DISCUSSION

The objective for the fiber optic sensor demonstration is to evaluate the sensor system potential to detect two different specific biomolecules with GNR and a stimuli responsive hydrogel independent from each other. The optical properties are then characterized first by recording the LSPR response to RI and the FSR as a function hydrogel swelling degree stimulated with pH. A relatively constant LSPR peak position as a function of hydrogel swelling degree would show that there is potential for utilizing the GNR for label free sensing that is independent of FSR measurements from the stimuli responsive hydrogel. On the contrary, a constant FSR as a function of bulk RI would show that there is potential for utilizing the stimuli responsive hydrogel for label free sensing that is independent from the LSPR measurements of local RI. Furthermore, the results would also show how this fiber optic system can be implemented in applications such as real-time monitoring of specific markers for critical ill patients under or after surgery[5,6]

3.1 Quality of the LSPR and interferometric measurements

The interferometric spectrum in figure 3a shows to have a shape of a low-finesse FP etalon as described in equation (1). Autocorrelation function was applied to the data from the interferometric spectrum to decrease noise. The autocorrelation coefficients with corresponding lag time in figure 3b was fitted with a sum of sinuses with 8 terms to find the trend and the peak positions. Peak 1 ,2 ,3... with corresponding lag times relates to the period of $\pi, 2\pi, 3\pi$... from the interferometric spectrum in figure 3a. FSR is then found from the peaks with corresponding lag times since it is directly scalable to the wavelength. It is possible to apply algorithms from

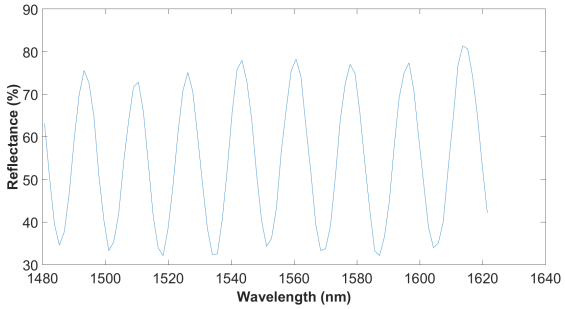

(a) IR reflection of GNR-hydrogel in mq water with pH 4.5

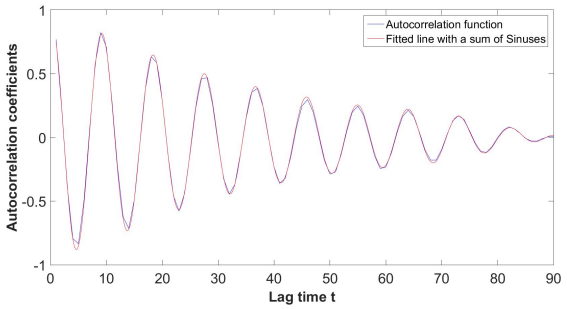

(b) Autocorrelation coefficients as a function of lag time from the IR reflection of GNR-hydrogel in mq water with pH 4.5

Figure 3: IR reflection of GNR-hydrogel in mq water with pH 4.5

previous work to obtain fast and accurate measurements from the same setup.[9,10] The VIS spectrum in figure 4 shows the LSPR from the GNR where the peak at 520nm and 687nm represents the transversal and longitudinal plasmon mode, respectively. The spectrum is fitted with a polynomial smoothing function with smoothing parameter at 0.999 that is centered and scaled. The longitudinal LSPR in figure 4 shows to be at 687nm while the longitudinal LSPR of GNR in citrate buffer (RI≈1.3301) is at 670nm. The redshift of longitudinal LSPR may be due to a local RI surrounding the GNR that is higher in the hydrogel than in the original citrate solution. The longitudinal LSPR is recorded for all pH and RI measurements since it has a higher absorption than the

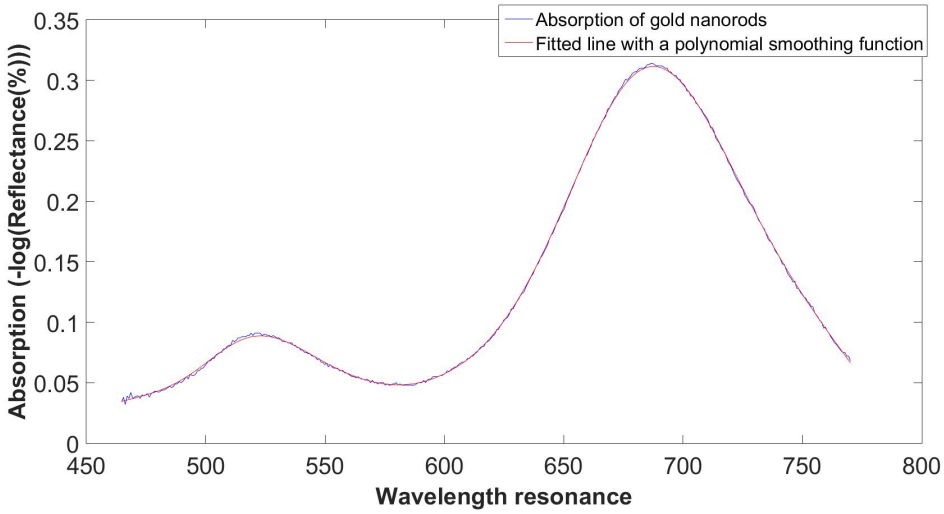

Figure 4: VIS absorption of GNR-hydrogel in mq water with pH 4.5

transverse LSPR.

3.2 LSPR and FSR measurements as a function of hydrogel swelling degree with pH

In figure 5 FSR is recorded for a series of pH changes from 4.5 to 3.5 and from 3.5 to 4.5 for two rounds.

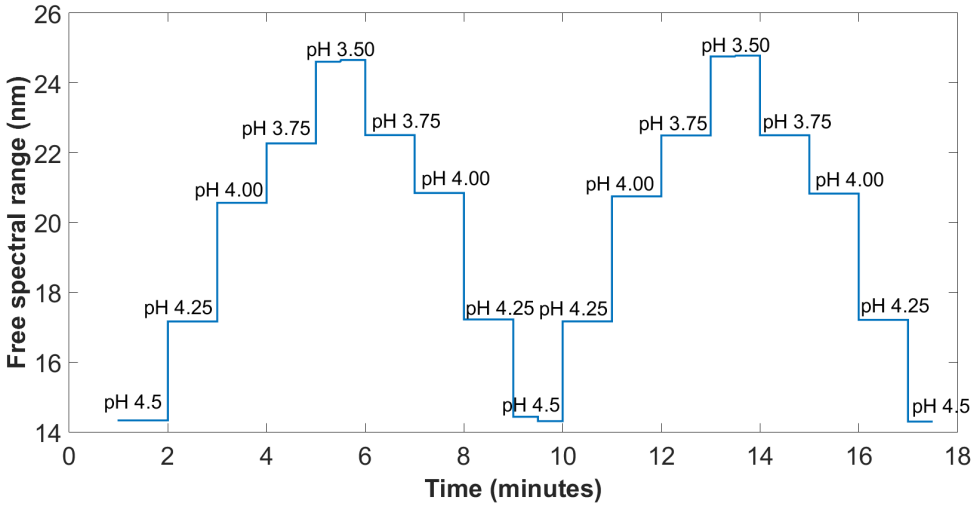

Figure 5: FSR measurements as a function hydrogel swelling degree stimulated by pH solutions

The FSR was recorded 1 minute after changing pH solution to ensure the hydrogel swelling or deswelling had reached equilibrium. Despite having GNR immobilized in the hydrogel, it is possible to have a repeatable read out of FSR as a function of hydrogel swelling degree. Experiments have shown that the visibility of the FP etalon is not decreasing for an increased amount of gold nanoparticles (GNP) in acrylamide gel.[11] Immobilizing GNR in the hydrogel introduces a loss factor with small absorption, scattering or mode mismatch coefficients. The mean and standard deviation of the collected FSR measurements from figure 5 are shown in figure 6.

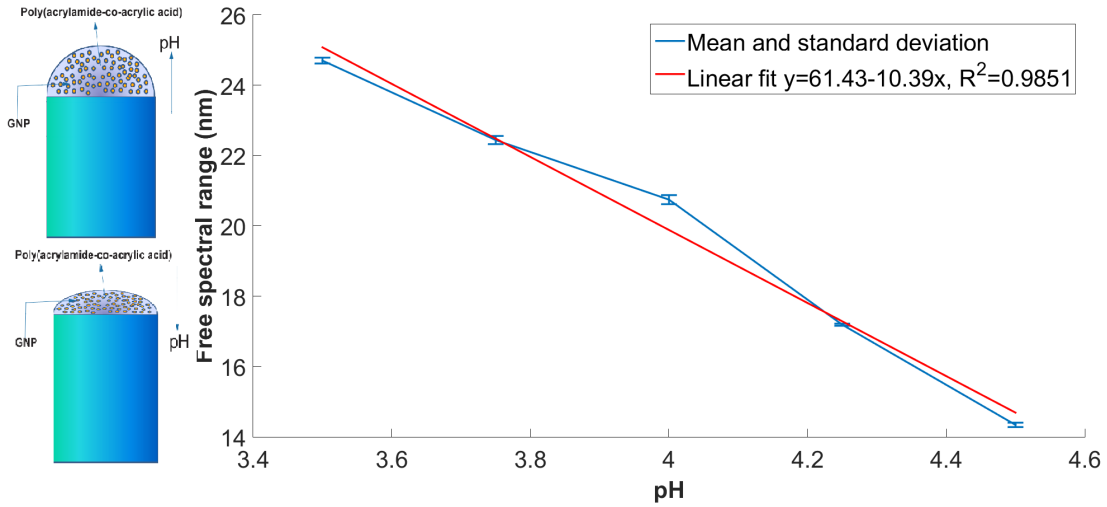

Figure 6: Mean and standard deviation of FSR as a function hydrogel swelling degree stimulated by pH solutions. The mean value and error bars are based on 4 measurements

The fitted line from the mean FSR shows to give a pH sensitivity of $\frac{\Delta \mathrm{pH}}{\Delta \mathrm{FSR}} = 0.09624/\mathrm{nm}$. The sensitivity towards pH depends on the ratio $\frac{\Delta \mathrm{Volume}}{\Delta \mathrm{pH}}$ of the pAAMAAC hydrogel and the resolution of the IR spectrometer. The

resolution for the spectrometer used in this FO system is ~ 1 nm. The range of pH that can be detected depends on same features as the sensitivity towards pH including the bandwidth of the light source and spectrometer. The range and sensitivity towards pH can be optimized by controlling the features mentioned above. Detecting the change in phase instead of FSR as described in previous work will also increase the sensitivity.[5,6,10] Mean and standard deviation of the LSPR measurements from figure 5 are shown in figure 7. The expected deswelling

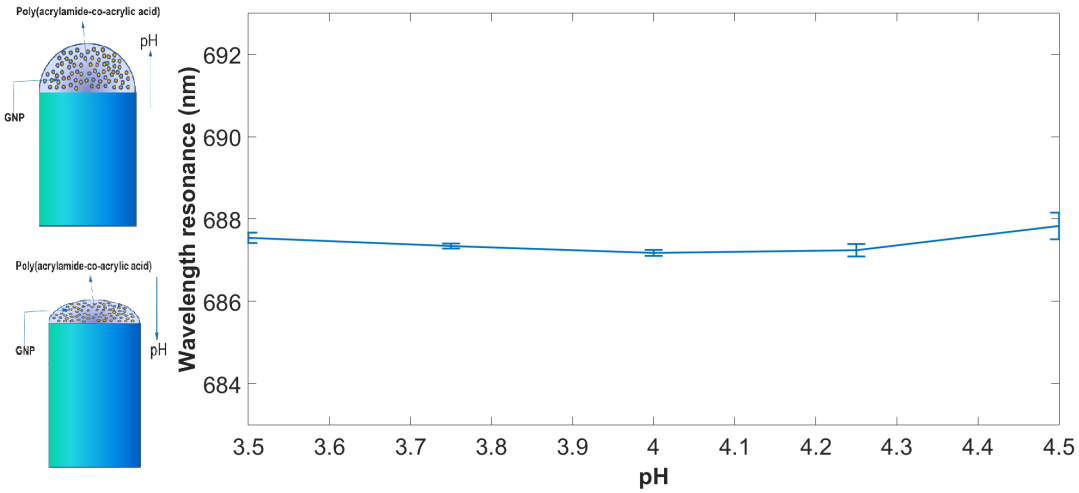

Figure 7: Mean and standard deviation of LSPR as a function hydrogel swelling degree stimulated by pH solutions. The mean value and error bars are based on 4 measurements

of pAAMAAC hydrogel results in an increase of RI around the GNR since the polymer network becomes denser. Previous work shows that the LSPR of 100nm spherical GNP can redshift with deswelling of pAAMAAC hydrogel as a result of an increase of RI in the gel or an electromagnetic interaction between the localized modes.[4] However, the LSPR measurements in figure 7 have a wavelength resonance that is changing between 688 and 687nm meaning that there is a negligible change of local RI or an electromagnetic interaction between the localized modes occurring between the individual GNR. The relatively constant wavelength resonance as a function of hydrogel swelling degree shows that there is potential for utilizing the GNR for label free sensing that is independent of the FSR measurements from a stimuli responsive hydrogel.

3.3 LSPR and FSR measuements as a function of bulk RI

The LSPR as a function of bulk RI and hydrogel swelling degree are shown in figure 8. The pH was controlled with HCl and NaOH for each of the bulk RI solutions of glycerol and sucrose. It is assumed that the bulk RI on the outside is the same as the inside of the hydrogel since glycerol and sucrose is water-soluble and therefore can be absorbed by the hydrogel with the water. Theoretically, the increase of bulk RI should lead to a redshift of the LSPR from the VIS reflection of GNR-pAAMAAC hydrogel. This is however not the case for the LSPR measurements in figure 8 where a blueshift is observed instead for the increased bulk RI. The LSPR shift is also non-linear having an increasing change of LSPR shift with increasing bulk RI. The total shift of LSPR with bulk RI is $\frac{\Delta\lambda_r}{\Delta \mathrm{RI}} \sim 877\mathrm{nm/RI}$. The blueshift for increased bulk RI is also observed for different swelling degrees of the hydrogel with pH as well as for the different chemicals of glycerol and sucrose. Considering that the pAAMAAC hydrogel contains a negatively charged acrylic acid co-monomer it may influence the orientation of the water-glycerol or water-sucrose molecules relative to the polymer network in the hydrogel resulting in a local RI that is different from the bulk RI. With bulk RI at 1.3848 the wavelength resonance is lower for glycerol and sucrose at low pH than for high pH indicating that the negatively charged acrylic acid may have an influence on the local refractive index surrounding the GNR for high wt% of glycerol or sucrose. If assuming a real $\frac{\Delta\lambda_r}{\Delta \mathrm{RI}} = 200\mathrm{nm/RI}$[12] for these particular GNR it will give a decrease in the local RI from 1.33 to $\sim$1.015. The GNR might also have an inhomogeneous distribution in the hydrogel as a result of the ionic strength and pH of the pregel solution

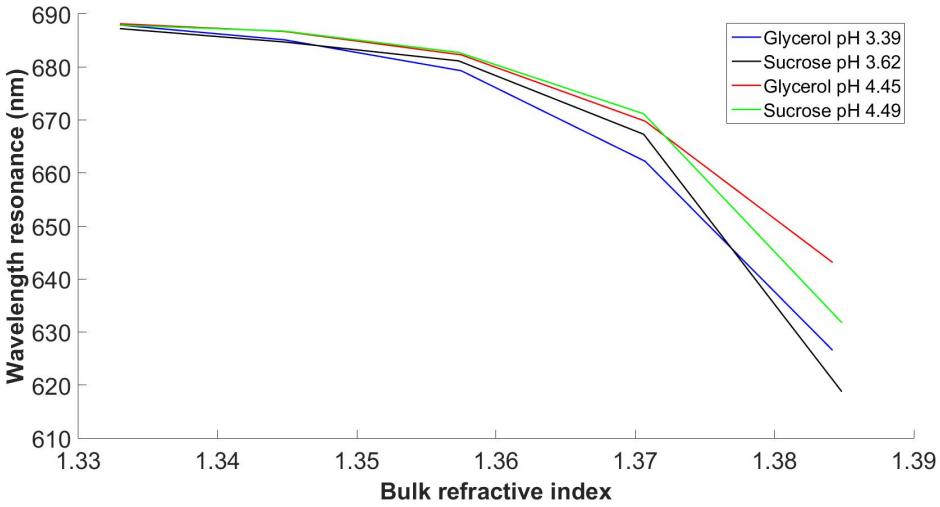

Figure 8: LSPR as a function of bulk RI for different pH solutions

or the polymerization process of the pregel. There is although little indication of aggregation of GNR as this should introduce a significant loss factor to the FP etalon reducing the visibility for the interferometric signal used in the measurements in section 3.1 and 3.2. *The local RI was measured in control experiments with biotin functionalized GNR in pAAMAAC hydrogel. The recombination of biotin-streptavidin showed a redshift of the LSPR. Another control measurements were obtained with GNR immobilized in AAM-BIS gel (10 wt% AAM, 2 mol% BIS) where the increase of bulk RI lead to a redshift of the LSPR. The control experiments enhance the validity of the assumption that the local RI could be different from the bulk RI. Further control and microscopy experiments will be conducted to pin point the fundamental model of the LSPR dependence from GNR-pAAMAAC hydrogel on RI with glycerol and sucrose. FSR measurements as a function of bulk RI for different pH solutions are shown in figure 9.

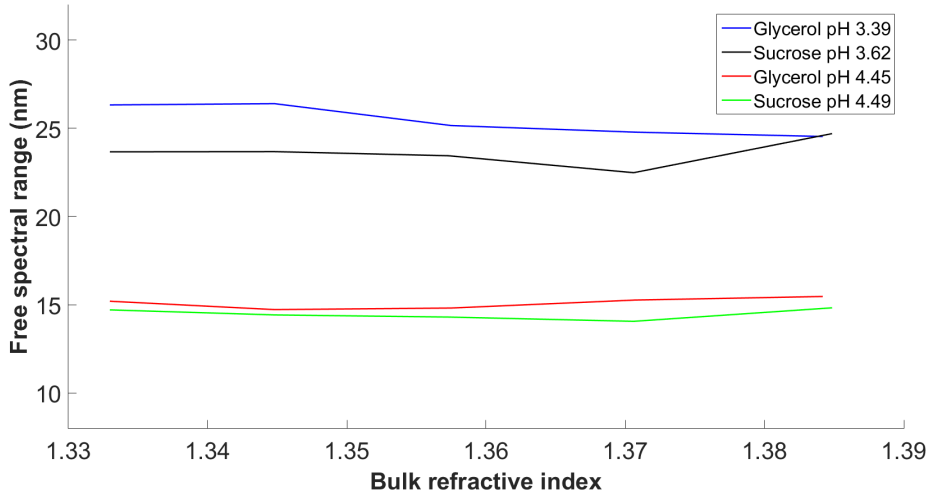

Figure 9: FSR as a function of bulk RI for different pH solutions

*Work in progress. To be published.

The FSR is not consistently increasing or decreasing with increasing bulk RI for high or low pH. If assuming the length l of the gel to be constant, the optical length should be proportional to the bulk RI. The FSR is inverse proportional to the optical length so an increase in bulk RI would lead to a decrease in FSR. Considering the change in optical length as described in equation (2), a negligible change in optical length Δl_0 could be due to a negative change in physical length Δl and a positive change in Δn. The change of physical length of the hydrogel was measured in an optical stereomicroscope (SZX7, Olympus) as a function og glycerol and sucrose at high and low pH. The estimated values are found in table 1. Δn_{gel} and initial n_{gel} is assumed to

Table 1: Estimated values of physical length and optical length. l_{02} represents optical length for mq water and glycerol or sucrose at bulk RI 1.3848 while l_{01} represents the optical length for mq water without glycerol or sucrose.

$\Delta wt\%$ solution	$\Delta l_0 = l_{02} - l_{01}$ from FSR eq. (3)	$\Delta l \cdot n_{\text{gel}}$	$\Delta n_{\text{gel}} \cdot l$	$\Delta l_0 = \Delta l n_{\text{gel}} + l\Delta n_{\text{gel}}$
Glycerol pH 4.45	-1.38μm	-2.8331μm	3.50μm	0.67μm
Sucrose pH 4.49	-0.64μm	-6.36μm	3.50μm	-2.86μm
Glycerol pH 3.39	3.33μm	-3.54μm	2.35μm	-1.19μm
Sucrose pH 3.62	-2.11μm	-2.71μm	2.35μm	-0.37μm

be 1.3848-1.3301=0.0547 and 1.3301, respectively. l values are obtained from the initial size of hydrogel in mq solutions at high and low pH values. The estimated Δl_0 from the measured FSR values are negative with exception of Glycerol pH 3.39. The estimated Δl_0 from the measured Δl are also negative with exception of Glycerol pH 4.45. In total the hydrogel deswelling has a higher impact than Δn_{gel} on the Δl_0 by changing from mq water to glycerol or sucrose solutions although the total change in Δl_0 is small. Small changes of FSR for bulk RI in figure 9 might then be a result of both the decrease of the hydrogel length l and the increase in n_{gel}.

Despite some uncertainties of the hydrogel deswelling degree concerning the optical length as a function of bulk RI and physical gel size, there is evidently a large response of LSPR for bulk RI in figure 8 and small response of FSR to bulk RI in figure 9. Taking also the results in section 3.2 into consideration, this proof-of-concept fiber optic sensor shows that we can sense the local RI and the pH stimulated hydrogel swelling degree simultaneously and relatively independent from each other. The results can be used to implement the label free sensor system for medical applications by tailoring the surface chemistry of the GNR and the hydrogel composition so it is possible to selectively real-time monitor specific biomolecules in a single point.[2,5,6,13]

4. CONCLUSION

FSR and LSPR were recorded from the reflection of GNR immobilized in pAAMAAC hydrogel on OF end-face as a function of pH and bulk RI. This novel proof-of-concept interferometric and nanoplasmonic FO sensor demonstrated that pH and bulk RI could be recorded simultaneously in one single point. The FSR were obtained from the interferometric measurements of hydrogel swelling degree stimulated by pH and showed a sensitivity of $\frac{\Delta \text{pH}}{\Delta \text{FSR}} = 0.09624/\text{nm}$. The LSPR measurements were relatively independent of the hydrogel swelling degree stimulated by pH with a wavelength resonance changing between ± 0.5nm. Glycerol or sucrose was used as bulk RI to characterize the sensitivity of LSPR from the GNR-pAAMAAC hydrogel. The wavelength resonance was blueshifting with increasing bulk RI in contrast to the fact that LSPR should redshift with increasing local RI. The local RI in the pAAMAAC hydrogel could be different from the bulk RI in glycerol or sucrose solutions. The blueshifting would in this case mean that the local RI is decreasing with increasing wt% of glycerol or sucrose in mq water. Control experiments demonstrated however a redshift for the recombination of biotin-streptavidin which indicates local RI sensing from the GNR. Changing the solution from mq water to glycerol or sucrose solutions resulted in a negligible change in FSR although the increase in RI should increase the optical length. The small change in FSR for wt% of glycerol or sucrose in mq water might be due to an optical length that is not only increased with RI but also decreased with hydrogel deswelling.

As this proof-of-concept represents a first step demonstration with purpose to characterize the function of the FP etalon and LSPR signal, it also shows how to sense pH and bulk refractive index simultaneously and independent of each other in a single point. Further work will be focused on demonstrating the FO system as a biosensor towards medical applications where specific markers will be detected.[2,5,6,13] The nanoplasmonic effects of noble metal nanoparticles immobilized in different hydrogels will also be focused on, as the LSPR features in hydrogel can be different from existing work on noble metal nanostructures on a surface or in a solution.

ACKNOWLEDGMENTS

This work was supported in part by the Interreg Sweden-Norway program (IR2015.01) and ENERSENSE (Strategic research program at Norweigan University of Science and Technology-Faculty of Science).

REFERENCES

[1] Mayer, K. M. and Hafner, J. H., "Localized surface plasmon resonance sensors," *Chem. Rev.* **111**, 3828–3857 (June 2011).

[2] Sanders, M., Lin, Y., Wei, J., Bono, T., and Lindquist, R. G., "An enhanced {LSPR} fiber-optic nanoprobe for ultrasensitive detection of protein biomarkers," *Biosensors and Bioelectronics* **61**(0), 95 – 101 (2014).

[3] Srivastava, S. K., Arora, V., Sapra, S., and Gupta, B. D., "Localized surface plasmon resonance-based fiber optic u-shaped biosensor for the detection of blood glucose," *Plasmonics* **7**(2), 261–268 (2011).

[4] Muri, H. I. D. I. and Hjelme, D. R., "Novel localized surface plasmon resonance based optical fiber sensor," **9702**, 97020L–97020L–8, SPIE (2016).

[5] Tierney, S., Falch, B. M. H., Hjelme, D. R., and Stokke, B. T., "Determination of glucose levels using a functionalized hydrogel optical fiber biosensor: Toward continuous monitoring of blood glucose in vivo," *Anal. Chem.* **81**, 3630–3636 (May 2009).

[6] Hjelme, D. R., Aune, O., Falch, B., Østling, D., and Ellingsen, R., "Fiber-optic biosensor technology for rapid, accurate and specific detection of enzymes," in [*Advanced Photonics*], *Advanced Photonics* , JTu6A.3, Optical Society of America (2014).

[7] Jensen, T. R., Duval, M. L., Kelly, K. L., Lazarides, A. A., Schatz, G. C., and Van Duyne, R. P., "Nanosphere lithography: Effect of the external dielectric medium on the surface plasmon resonance spectrum of a periodic array of silver nanoparticles," *J. Phys. Chem. B* **103**, 9846–9853 (Nov. 1999).

[8] Haynes, W. M., [*Handbook of Chemistry and Physics 97th edition*], CRC Taylor and Francis Group (2016-2017).

[9] Bartholsen, I. and Hjelme, D. R., "Fast and accurate read-out of interferometric optical fiber sensors," **9754**, 97540E–97540E–7, SPIE (2016).

[10] Tierney, S., Hjelme, D. R., and Stokke, B. T., "Determination of swelling of responsive gels with nanometer resolution. fiber-optic based platform for hydrogels as signal transducers," *Anal. Chem.* **80**, 5086–5093 (July 2008).

[11] Muri, H. I. D. I., Bano, A., and Hjelme, D. R., "First step towards an interferometric and localized surface plasmon fiber optic sensor, paper number: Ofs100-046," in [*25th International Conference on Optical Fiber Sensors (OFS-25), Chemical, Environmental, Biological and Medical Sensors and Biophotonics*], (2017).

[12] Chen, H., Kou, X., Yang, Z., Ni, W., and Wang, J., "Shape- and size-dependent refractive index sensitivity of gold nanoparticles," *Langmuir* **24**, 5233–5237 (May 2008).

[13] Jeong, H.-H., Erdene, N., Park, J.-H., Jeong, D.-H., Lee, H.-Y., and Lee, S.-K., "Real-time label-free immunoassay of interferon-gamma and prostate-specific antigen using a fiber-optic localized surface plasmon resonance sensor," *Biosensors and Bioelectronics* **39**, 346–351 (Jan. 2013).